3-26-2019

Mechanical properties of Michigan Basin's gypsum before and after saturation

Mohammadhossein Sadeghiamirshahidi
Michigan Technological University, msadeghi@mtu.edu

Stanley Vitton
Michigan Technological University, vitton@mtu.edu

Recommended Citation

Sadeghiamirshahidi, M., & Vitton, S. (2019). Mechanical properties of Michigan Basin's gypsum before and after saturation. *Journal of Rock Mechanics and Geotechnical Engineering, 11*(4), 739-748. http://doi.org/10.1016/j.jrmge.2018.10.006
Retrieved from: https://digitalcommons.mtu.edu/michigantech-p/430

Follow this and additional works at: https://digitalcommons.mtu.edu/michigantech-p

 Part of the Civil and Environmental Engineering Commons

Journal of Rock Mechanics and Geotechnical Engineering 11 (2019) 739–748

Contents lists available at ScienceDirect

Journal of Rock Mechanics and Geotechnical Engineering

journal homepage: www.rockgeotech.org

Full Length Article

Mechanical properties of Michigan Basin's gypsum before and after saturation

Mohammadhossein Sadeghiamirshahidi*, Stanley J. Vitton

Department of Civil and Environmental Engineering, Michigan Technological University, Houghton, MI, USA

ARTICLE INFO

Article history:
Received 16 May 2018
Received in revised form
5 September 2018
Accepted 23 October 2018
Available online 26 March 2019

Keywords:
Uniaxial compressive strength (UCS)
Brazilian tensile strength (BTS)
Point load index (PLI)
Scale effect
Michigan Basin's gypsum

ABSTRACT

The stability analysis of an abandoned underground gypsum mine requires the determination of the mine pillar's strength. This is especially important for flooded abandoned mines where the gypsum pillars become saturated and are subjected to dissolution after flooding. Further, mine pillars are subjected to blast vibrations that generate some level of macro- and micro-fracturing. Testing samples of gypsum must, therefore, simulate these conditions as close as possible. In this research, the strength of gypsum is investigated in an as-received saturated condition using uniaxial compressive strength (UCS), Brazilian tensile strength (BTS) and point load index (PLI) tests. The scale effect was investigated and new correlations were derived to describe the effect of sample size on both UCS and BTS under dry and saturated conditions. Effects of blasting on these parameters were observed and the importance of choosing the proper samples was discussed. Finally, correlations were derived for both compressive and tensile strengths under dry and saturated conditions from the PLI test results, which are commonly used as a simple substitute for the indirect determination of UCS and BTS.

1. Introduction

Determining the mechanical properties of gypsum rock is important in many engineering projects including the stability of abandoned underground gypsum mines, especially for mines that become flooded after mining operations have been completed (Doulati Ardejani et al., 2013). Uniaxial compressive strength (UCS) is one of the most widely used rock parameters in design and stability analyses (Xie et al., 2011; Munoz and Taheri, 2017; Salehin, 2017; Salih and Mohammed, 2017; Marolt Čebašek and Frühwirt, 2018). This parameter is commonly measured in laboratory using specifically sized cylindrical samples selected from intact cores. Despite the importance of sample size and its effect on the rock's UCS, it is not always possible to prepare samples that meet the required standards, mainly due to the time-consuming and expensive process of sample preparation. The American Society for Testing and Materials (ASTM) recognizes this problem and allows samples with sizes outside the proposed range provided that "suitable notation" is made to report the actual size of samples. In these cases, however, the corrected UCS still needs to be determined (using the scale effect analyses) in stability analyses. Although scale effect has been studied for different rocks (e.g. Hoek and Brown, 1980; Yoshinaka et al., 2008), it is important to investigate this effect for gypsum rocks, in order to use the results of different sized samples where standard samples are not available. Correlations derived from scale effect analyses can also be used to investigate the existence of micro-flaws in samples (Yoshinaka et al., 2008). Micro-flaws in the rocks can form naturally or be caused by mining activities such as blasting used in underground mines or quarries.

An alternative approach to avoid time-consuming and expensive sample preparation for UCS is to use indirect methods such as point load index (PLI) tests to determine the UCS. Although PLI tests can be conducted axially and diametrically on cylindrical samples as well as on samples with irregular shapes, the diametrical tests on cylindrical samples are considered more reliable and are commonly used in design (e.g. Bieniawski, 1975; Chau, 1998; Heidari et al., 2012). PLI tests will not, however, eliminate the need for UCS tests as, despite extensive research on the correlations between PLI and UCS, the empirical correlations are specific to each rock type and should be experimentally established for different rock types.

Another important parameter in the stability analysis of underground mines is the roof rock's tensile strength. It is difficult to

* Corresponding author.
E-mail address: msadeghi@mtu.edu (M. Sadeghiamirshahidi).
Peer review under responsibility of Institute of Rock and Soil Mechanics, Chinese Academy of Sciences.

https://doi.org/10.1016/j.jrmge.2018.10.006

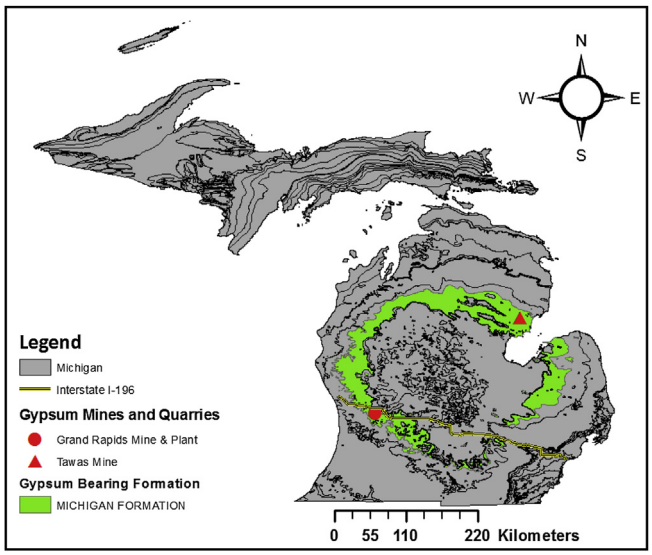

Fig. 1. Study area (Map was developed using ArcMap version 10.5.1, and the data for developing the map were obtained from USGS (accessed: 4/2/2018)).

measure the tensile strength of rock directly, thus an indirect method, i.e. the splitting tensile strength test (commonly known as Brazilian tensile strength (BTS) test), is used. The accuracy of the BTS test, however, is somewhat compromised due to excessive stress concentrations at load contact points (Wong and Jong, 2014). Modifications are offered to reduce these stress concentrations such as using curved platens or curved spacers (Yu et al., 2009). According to ASTM, both modifications are acceptable, but they recommend using bearing cardboard strips with a thickness of 0.01 times the sample diameter between the sample and loading platen. BTS of rocks can also be estimated from PLI if the correlation between BTS and PLI is known.

Finally, in flooded abandoned mines, pillars that were unsaturated during mining operations become saturated. Although the effect of saturation on gypsum strength has been studied (e.g. Lisk, 1975; Ali, 1979; Doktan, 1983; Hoxha et al., 2006; Castellanza et al., 2007; Yilmaz, 2010; Heidari et al., 2012), there is a wide range of results regarding the magnitude of the strength loss due to saturation. For example, a 22% reduction in UCS of gypsum was reported by Lisk (1975), while Ali (1979) reported a reduction of 47%–49%. Further, Doktan (1983) tested gypsum samples from two areas and reported a 25% reduction in UCS of samples from one location and a 42% reduction in the second area. Doktan (1983) qualitatively attributed the differences between the two locations to different fabrics, compositions, grain sizes and weathering states of the rocks. Gypsum samples tested by Preston (1980) were obtained from different sources as well and showed 25.5%, 25.9%, 35% and 42.2% reductions in UCS after saturation. Doktan (1983) and Preston (1980) both reported that the highest reductions of strength were observed in the samples with the coarsest grains. Heidari et al. (2012) tested air-dried and saturated samples from Gachsaran formation in Iran and their results showed an average of 31.5% reduction in strength due to saturation. While these results showed a strength reduction due to saturation, the quantitative value of reduction varies significantly from case to case, suggesting that the strength reduction should be determined experimentally for each project location.

In this study, the mechanical properties of Michigan Basin's gypsum and the effects of sample size, blasting and saturation on these properties were investigated. This was necessary for the stability analysis of an abandoned gypsum mine in Michigan, which is located under a busy highway. The main objectives of this study were (i) to determine the mechanical properties of Michigan Basin's gypsum and understand the scale effect on its compressive and tensile strengths by developing equations correlating sample size with UCS and BTS, (ii) to determine the effect of blasting on UCS of gypsum, (iii) to understand the effect of saturation on mechanical properties (UCS, elasticity moduli, BTS and PLI) of gypsum determined by testing dry and saturated samples, and (iv) finally to establish correlations between PLI, UCS and BTS.

2. Site location, materials and methods

This study is part of a project concerning the stability of the Domtar mine, an abandoned underground gypsum mine near Grand Rapids, Michigan, USA (Fig. 1). About 640 m of a busy highway (Interstate I-196) pass directly over a northeast portion of the mine located at a depth of about 30 m below I-196. Over the mine's life, subsidence and sinkholes have formed, raising concerns about the long-term stability of the mine, especially under I-196. The 3.5 m thick gypsum seam had been mined for over 150 years ending in 2000. While the underground gypsum mines in the Michigan Basin are now closed, there are two operating quarries located near Tawas City, on the east side of the state, adjacent to Lake Huron. The gypsum seam is part of Michigan formation (Mississippian Age) in the Michigan Basin. After mining ended in 2000, the mine was reported to be flooded by 2003 (Vitton, 2004). Since the mine is flooded, our access to collect samples for testing was limited and therefore samples from Tawas quarry (shown in Fig. 1), which belongs to the same formation (Grimsley, 1904), were used for this research.

Fig. 2. Apparatuses used in the laboratory for (a) UCS, (b) BTS, (c) PLI, and (d) parallelism measurement.

Table 1
Results of carbonate content tests.

Sample ID	Description	$CaCO_3$ (wt%)
CC1	Pink with some gray impurities	2.14
CC2	Significant gray impurities	8.16
CC3	Pink with some gray impurities	2.73
CC4	Significant gray impurities	5.49
CC5	Significant gray impurities	9.52
CC6	White	1.3
CC7	White	1.3

Table 2
Summary of PXRF results.

Sample ID	Description	S (wt%)	Ca (wt%)	Fe (wt%)	Sr (wt%)
PXRF1	White	52.27	32.73	0.01	0.09
PXRF2	Gray	23.68	35.57	0.74	0.23
PXRF3	White	54.78	34.19	0.01	0.09
PXRF4	Pink	50.96	31.81	0.01	0.03
PXRF5	Gray	47.88	34.9	0.06	0.03
PXRF6	Pink	53.16	33.07	0.01	0.09
PXRF7	Pinkish white	48.84	32.23	0.02	0.12
PXRF8	Dissolved in flowing water for 24 h, and then oven-dried at 105 °C for 48 h	61.75	36.94	0.02	0.08

Gypsum blocks were obtained from the National City Quarry near Tawas, Michigan and transported to the Rock Mechanics Laboratory at Michigan Technological University. Samples were cored at the following three diameters: (a) 2.8 cm (1.1 in), (b) 5.4 cm (2.1 in) and (c) 7.6 cm (3 in). Following coring, the samples were cut on a diamond saw to a height (H) to diameter (D) ratio of $H/D \geq 2.1$. An attempt was made to grind the core surfaces but was unsuccessful due to gypsum dissolution and breakage of the samples during grinding. The parallelism of the samples, however, was measured using the device shown in Fig. 2d, to make sure that they are in an acceptable range. Half of the prepared samples were air-dried for eight weeks before testing, while the other half were saturated using the methods discussed in Sadeghiamirshahidi and Vitton (2019a). The samples that broke during surface grinding or the ones that did not meet the parallelism requirements were either used for dissolution tests (as discussed in Sadeghiamirshahidi and Vitton, 2019b), and they were cut to smaller samples for PLI tests, or to disks for BTS. Half of these samples were also air-dried while the other half were saturated before testing started.

Gypsum samples with different diameters were prepared to investigate the effect of sample size on strength parameters. Hoek and Brown (1980) addressed the importance of sample size and provided a correlation between sample size and a dimensionless form of UCS as follows:

$$UCS/UCS_{(50)} = (50/D)^{0.18} \quad (1)$$

where $UCS_{(50)}$ is the UCS of samples with a diameter (D) of 50 mm, and D is the diameter of samples in mm (Hoek and Brown, 1980). The correlation is based on published experimental results for different rock types. Because the relationship is based on various rock types, there can be a difference between the actual strength and the strength predicted by the correlation for some rock types. Other researchers have also developed similar but improved correlations, among which Eq. (2) proposed by Yoshinaka et al. (2008) is one of the more common correlations:

$$UCS/UCS_{(50)} = (d_e/d_{e50})^{-k} \quad (2)$$

where d_e is the equivalent length (which is defined as the cube root of the sample volume), d_{e50} is the equivalent length of the standard sample ($D = 50$ mm), and k is a material constant that depends on rock type (hard or soft) and the presence or absence of rock microflaws. They categorized rocks into two groups, i.e. soft rocks with UCS less than 25 MPa, and hard rocks with UCS greater than 25 MPa. Based on their laboratory and in situ test results, they concluded that k can vary from 0.1 to 0.3 for the hard rock without

Table 3
Summary of UCS test results on dry samples.

Sample ID	Diameter (mm)	Dry *UCS* (MPa)	Tangent modulus (GPa)	Secant modulus (GPa)	Average modulus of linear portion of axial stress-strain curve (GPa)	Failure mode	Dry $UCS_{(54)}$ (MPa)
DRY-1	28.24	29.14	2.75	1.51	3.99	Axial splitting	17.6
DRY-2	28.27	30.64	3.42	1.62	3.75	Axial splitting	18.53
DRY-3	28.26	26.21	3.67	1.67	3.65	Axial splitting	15.84
DRY-4	28.23	25.1	2.79	1.57	4.35	Axial splitting	15.16
DRY-5	28.22	48.31	6.31	2.76	7	Shearing along single plane	29.17
DRY-6	28.25	43.97	5.86	2.45	6.77	Shearing along single plane	26.58
DRY-7	28.21	11.97	1.1	0.57	0.99	Axial splitting	7.22
DRY-8	28.27	15.93	1.35	0.81	1.15	Axial splitting	9.63
DRY-9	28.31	34.68	4.08	1.91	4.53	Axial splitting	20.99
DRY-10	28.33	37.54	4	1.65	4.07	Multiple fracturing	22.74
DRY-11	28.37	38.49	5.24	2.76	7.65	Multiple fracturing	23.35
DRY-12	53.03	23.95	4.3	2.55	4.28	Multiple fracturing	24.15
DRY-13	53.95	11.35	2.15	1.31	2.27	Axial splitting	11.61
DRY-14	54.07	14.76	2.76	1.36	4.51	Shearing along single plane	15.12
DRY-15	54.04	16.28	3.81	1.74	3.67	Shearing along single plane	16.67
DRY-16	54.1	26.94	4.96	2.49	5.46	Multiple fracturing	27.62
DRY-17	75.71	20.85	6.61	2.53	7	Y-shaped	28.08
DRY-18	75.78	11.84	2.73	1.63	2.77	Shearing along single plane	15.96
DRY-19	75.77	14.17	4.05	2.03	4.48	Shearing along single plane	19.09
DRY-20	75.82	14	4.13	2	4.47	Shearing along single plane	18.88
DRY-21	75.82	14.72	1.99	1.04	3.43	Multiple fracturing	19.86
DRY-22	75.65	8.78	2.22	0.93	2.06	Shearing along single plane	11.82
DRY-23	75.7	12.81	4.39	1.79	5.13	Shearing along single plane	17.26

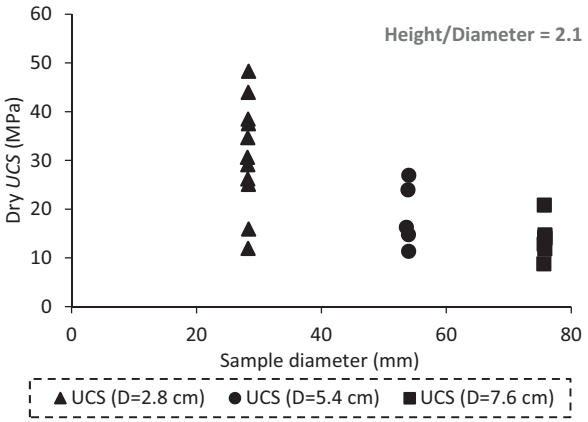

Fig. 3. UCS of air-dried samples with different sizes.

micro-flaws and from 0.3 to 0.9 for highly micro-flawed hard rock, while it is always less than 0.5 for soft rocks (Yoshinaka et al., 2008). These micro-flaws in the rocks can be formed during natural geologic processes or caused by blasting operations in underground mines or surface quarries. In the early stages of mine design, the UCS is usually measured from cores from a drilling program not subjected to blasting. This can result in overestimating the strength of pillars when blasting is used as part of the mining operations.

After the sample preparations, UCS values of dry and saturated samples were measured according to ASTM D7012-14 (2014) using a MTS stiff frame servo-hydraulic compression machine with a top bearing platen, as shown in Fig. 2a. The UCS values of samples, as well as all three types of elasticity moduli (secant, tangent and average slope of linear portion of stress-strain curve), were calculated for both dry and saturated samples. A MTS mechanical compression machine (Fig. 2b) was used for BTS testing, and a portable point load testing machine (Fig. 2c) was used to conduct the PLI tests. Both BTS and PLI tests were conducted on dry and saturated samples, according to ASTM D3967-16 (2016) and ASTM D5731-16 (2016), respectively. For PLI tests, however, only samples with diameter of 2.8 cm were tested. In addition, a portable X-ray fluorescence (PXRF) analyzer was used to study the composition of the gypsum. Each sample was scanned three times (each time for 30 s) using the soil mode which is the optimized option for detecting lighter elements (Ca, K, S, P, Cl and I). Finally, carbonate content (calcite equivalent) of the samples was measured according to ASTM D4373-14 (2014) using hydrochloric acid (HCl) in an enclosed reaction cylinder.

3. Results and discussion

3.1. Gypsum composition results

Gypsum samples from Tawas quarry had two distinctive white and pink colors along with secondary gray impurities. To determine the composition of samples, carbonate content tests were conducted on the samples. The test results are summarized in Table 1. As can be seen, the samples with the higher gray impurities had the highest carbonate content (about 8%–10%), while the white and pink samples with little or no gray impurities had the lowest carbonate contents of about 1%.

The PXRF results of eight samples, which determine the percentage by weight of the main chemical components, are listed in Table 2. The samples were scanned to determine the composition of the materials in three colors. While calcium (Ca) can be from either gypsum or calcium carbonates, sulfur (S) would represent gypsum. As can be seen, the percentage by weight of sulfur (S) is lower for gray areas showing a higher percentage of carbonate which is in agreement with the carbonate content test results. The PXRF results also indicate that the composition of all samples is relatively consistent.

3.2. Uniaxial compression test results

The UCS values of air-dried samples with different sizes are summarized in Table 3. To better indicate the relationship between sample size and UCS, the UCS values of samples are plotted against sample diameter in Fig. 3. It can be seen from this figure that, as expected, larger samples have lower strengths. This is generally believed to be due to a larger amount of flaws existing in larger samples. Fig. 3 also shows, however, a larger scatter in the data for smaller samples compared to the larger samples. One possibility for this larger scatter might be due to production blasting causing a higher percentage of micro-factures in the gypsum. While there is a chance of obtaining a small sample with minimum to no cracks (flaws) from blasted rocks, there still might be some small samples with some cracks (Fig. 4). For larger samples, on the other hand, cracks most likely exist in the sample (Fig. 4). Therefore, since the number of flaws controls the strength of rock, small samples show more substantial variance from the average. To further investigate this issue, the average UCS for each sample size was calculated and plotted on the chart developed by Hoek and Brown (1980), as shown in Fig. 5. To develop this chart, the data presented by Hoek and Brown (1980) were approximated using PlotDigitizer (version 2.6.8) and plotted along with our results. Hoek and Brown (1980) used samples with $D = 50$ mm as their reference (standard) and

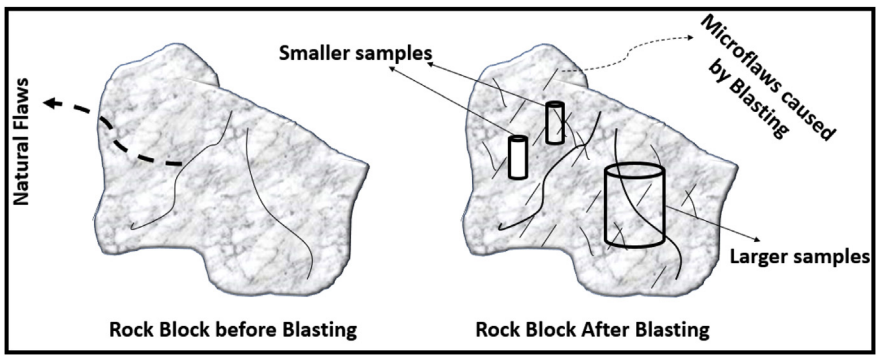

Fig. 4. Schematic demonstration of flaws in a rock block before and after blasting and its effect on core samples.

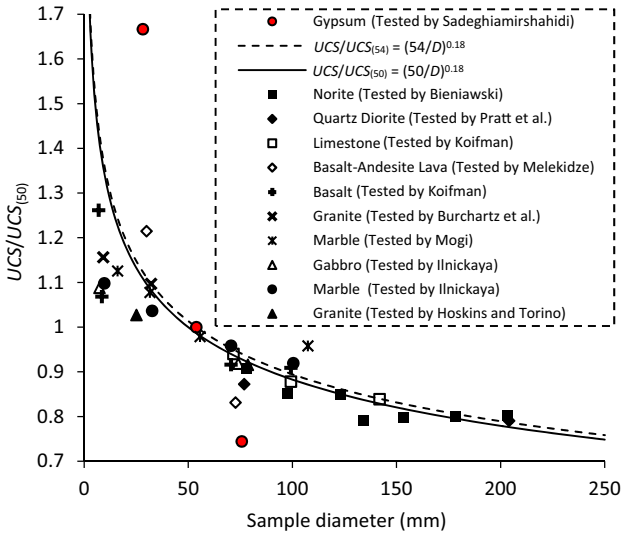

Fig. 5. Average of UCSs for gypsum with different sizes (plotted on Hoek and Brown (1980)'s chart).

developed Eq. (1) which is also included in Fig. 5. As the closest diameter in our tests to their standard diameter was 54 mm, we also plotted the Hoek-Brown (1980)'s equation using $D = 54$ mm as the reference which is shown with dashed line in Fig. 5. As can be seen from this figure, the two curves are very close, suggesting that the change of reference diameter from 50 mm to 54 mm does not significantly affect the results. This allows us to develop a similar equation for Michigan Basin's gypsum using the UCS of samples with $D = 54$ mm ($UCS_{(54)}$) as the reference, as shown in Fig. 6. As for a similar equation to the Hoek-Brown equation (Eq. (1)), only changing the exponent in the equation to 0.81 can well describe the effects of sample size on the strength of Michigan Basin's gypsum.

Eq. (2) developed by Yoshinaka et al. (2008) was also used, where $k = 0.81$ was employed to fit our results, as shown in Fig. 6. According to the criterion provided by Yoshinaka et al. (2008), having k in the range of 0.3–0.9 represents highly micro-flawed hard rock which further suggests the possible effects of blasting on our samples.

The UCS values of saturated samples with different sizes were also measured, and the test results are summarized in Table 4. The relations between sample size and UCS are shown in Fig. 7. The same charts showing the size effect for saturated samples are plotted in Fig. 8. For saturated gypsum, the exponent in Eq. (1) was calculated to be 0.72 (Fig. 8) and k in Eq. (2) was 0.72 which again suggested the micro-flawed condition of samples due to blasting. The comparison between saturated and air-dried samples shown in Fig. 9 indicates a 41% reduction in UCS after saturation. It is worth mentioning that for both saturated and dry samples, larger samples ($D > 2.8$ cm) retained some residual strength after failure, meaning that the failure was not as brittle as shown in Fig. 10a, but almost all of the small samples ($D = 2.8$ cm) had abrupt brittle failures (Fig. 10b).

Three types of elasticity moduli (Fig. 10) were calculated for all samples (dry and saturated), and the averages are tabulated in Table 5. The results show that the elasticity moduli were reduced by 30%–50% after saturation. Four types of failure modes, i.e. axial splitting (Fig. 11a), single shear (Fig. 11b), multiple fracturing (Fig. 11c), and Y-shaped failure (Fig. 11d), were observed in dry

Table 4
Summary of UCS test results for saturated samples.

Sample ID	Diameter (mm)	Saturated *UCS* (MPa)	Tangent modulus (GPa)	Secant modulus (GPa)	Average modulus of linear portion of axial stress-strain curve (GPa)	Saturated $UCS_{(54)}$ (MPa)
SAT-1	28.24	14.26	1.23	0.91	2.5	8.56
SAT-2	28.27	15.34	2.25	1.51	3	9.21
SAT-3	28.26	15.78	1.99	1.61	2.02	9.47
SAT-4	28.23	13.34	1.83	1.23	2.02	8
SAT-5	28.22	23.29	3.12	1.92	3.34	13.97
SAT-6	28.25	20	3.69	2.33	4.18	12.01
SAT-7	28.21	8.84	0.72	0.88	0.98	5.3
SAT-8	28.27	11.56	0.61	0.47	1.12	6.94
SAT-9	28.31	14.9	1.1	1.01	2.21	8.96
SAT-10	28.33	27.09	3.2	2.03	3.97	16.29
SAT-11	28.37	30.25	3.15	2.01	3.76	18.21
SAT-12	53.03	9.94	1.36	0.8	1.96	9.39
SAT-13	53.95	9.9	1	0.88	2.62	9.47
SAT-14	54.07	10.06	1.37	0.9	2.45	9.63
SAT-15	54.04	9.34	0.18	0.36	0.43	8.94
SAT-16	54.1	12.96	0.74	0.49	1.02	12.42
SAT-17	75.71	10.87	1.45	1.64	2.76	13.27
SAT-18	75.78	11.13	2.33	1.23	4.41	13.6
SAT-19	75.77	6.07	2.23	1.35	2.21	7.41
SAT-20	75.82	7.73	2.76	1.78	3.34	9.44
SAT-21	75.65	7.11	2.24	1.54	2.82	8.67
SAT-22	75.7	9.97	2.28	1.46	2.5	12.17

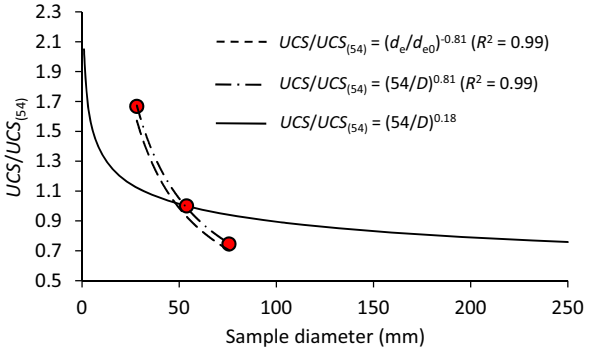

Fig. 6. Different criteria developed to describe the influence of sample size on UCS of air-dried natural gypsum from Michigan Basin.

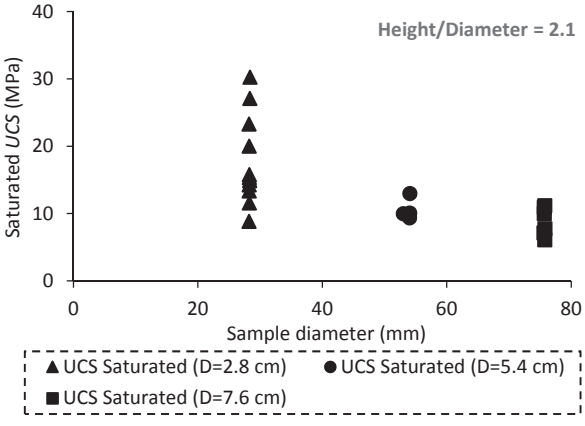

Fig. 7. UCS of saturated samples with different sizes.

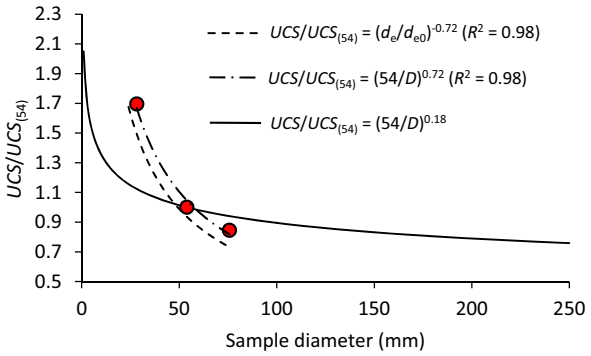

Fig. 8. Different criteria developed to describe the influence of sample size on UCS of saturated natural gypsum from Michigan Basin.

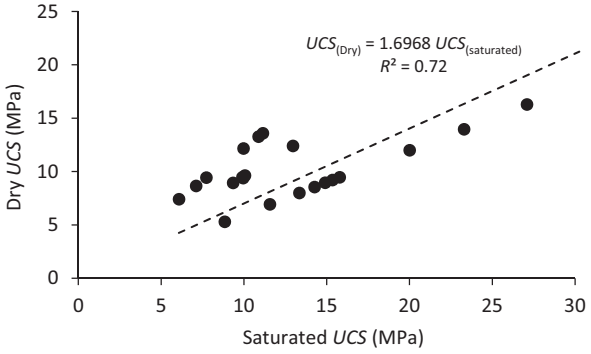

Fig. 9. Comparison between air-dried and saturated UCS values.

samples, but in saturated samples, almost all failed along a single shear plane. Despite hypotheses in the literature trying to explain various failure modes for example by using damage evolution of the rocks and correlating the failure mode to strength or sample size as explained by Basu et al. (2013), no such correlation could be established for gypsum tested in this research. The lack of correlation might possibly be due to the level of micro-fractures caused by production blasting.

3.3. Point load index test results

The results of PLI tests on dry and saturated samples are summarized in Table 6. To derive a correlation between UCS and PLI, the results of PLI tests (I_{S50}) for both dry and saturated samples have been plotted versus UCS test results, as shown in Figs. 12 and 13, respectively. It should be noted that the UCS results were converted to $UCS_{(54)}$ using Eq. (3) for dry samples and Eq. (4) for saturated samples that were previously derived for Michigan Basin's gypsum (Figs. 6 and 8, respectively) before plotting against I_{s50}:

$$UCS/UCS_{(54)} = (54/D)^{0.81} \quad (3)$$

$$UCS/UCS_{(54)} = (54/D)^{0.72} \quad (4)$$

It should also be noted that the trend lines were forced to pass through zero as the authors believe that having an arbitrary constant (y-intercept) without any physical explanation in the equation is unwarranted. Furthermore, forcing the trend line through the origin did not significantly reduce the coefficient of determination, R^2. Also, the definition used by ASTM D5731-16 (2016) (general form of $UCS = KI_{s50}$) for "PLI to UCS conversion factor (K)" does not include any arbitrary y-intercept. It is also important to mention that, to develop these charts, all the UCS and PLI results were sorted from lowest to highest and plotted against each other. The index to strength conversion factor K was 6.6 for dry samples and 7.7 for saturated samples.

3.4. Brazilian tensile strength test results

Indirect tensile strengths of air-dried samples with three diameters were measured using BTS tests. The results are summarized in Table 7, and the relations between sample size and BTS are provided in Fig. 14. It can be seen from Fig. 14 that the BTS results also decrease with increasing sample size, but in this case, the scatter of results for all sizes is similar. This is because samples in BTS tests, compared to UCS samples, are smaller and the possibility of having intact samples or samples with some micro-flaws is relatively similar for all three sizes.

An attempt was made to develop a criterion explaining the relationship between sample size and BTS, as shown in Fig. 15. The coefficient of determination (R^2) for this data set is about 0.86, which is lower than that for UCS (about 0.99). It is suggested that the wider range of thickness to diameter ratios used in these tests (0.3–0.7) might account for this decrease, since the range of sample height to diameter ratio for UCS was relatively constant around 2.1 (2.04–2.2). Unfortunately, a larger number of samples with different diameters were not available to determine such a relationship for saturated BTS.

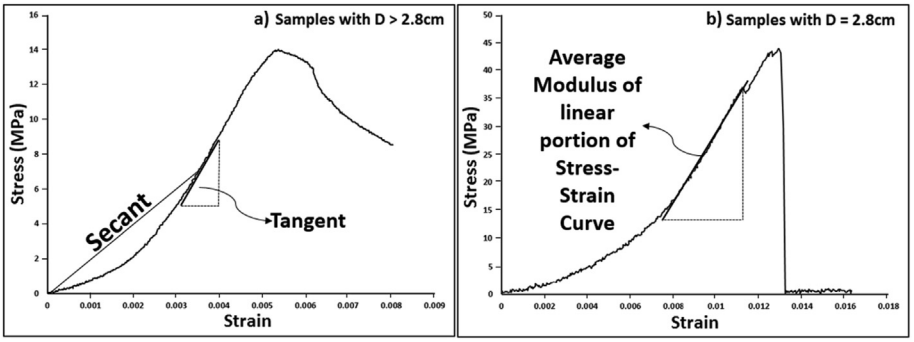

Fig. 10. Two typical types of stress-strain curves obtained for gypsum samples tested in this study.

Table 5
Three types of elasticity moduli calculated for dry and saturated samples.

Sample	Secant modulus (GPa)	Tangent modulus (GPa)	Average modulus of linear portion of axial stress-strain curve (GPa)
Air-dried	1.77	3.68	4.11
Saturated	1.2	1.86	2.53

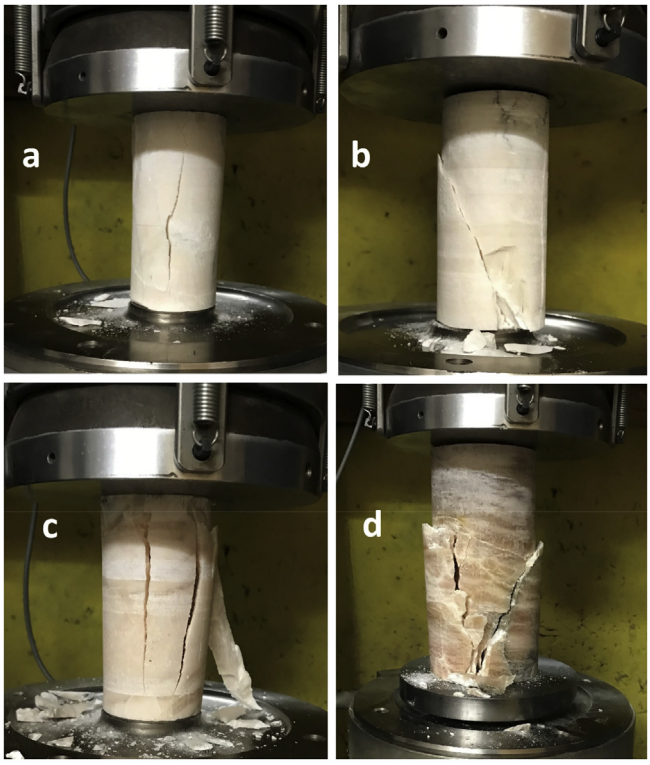

Fig. 11. Failure modes observed in UCS testing on Michigan Basin's gypsum: (a) Axial splitting, (b) Single shear, (c) Multiple fracturing, and (d) Y-shaped failure.

Table 6
Summary of PLI test results for dry and saturated samples.

Sample	ID	I_{s50} (MPa)
Air-dried	IsDRY-1	1.14
	IsDRY-2	1.69
	IsDRY-3	1.69
	IsDRY-4	1.73
	IsDRY-5	1.78
	IsDRY-6	1.79
	IsDRY-7	1.84
	IsDRY-8	2.49
	IsDRY-9	2.73
	IsDRY-10	2.78
	IsDRY-11	2.99
	IsDRY-12	3
	IsDRY-13	3.03
	IsDRY-14	3.14
	IsDRY-15	4.19
Saturated	IsSAT-1	0.7
	IsSAT-2	0.8
	IsSAT-3	0.84
	IsSAT-4	0.88
	IsSAT-5	1.14
	IsSAT-6	1.17
	IsSAT-7	1.17
	IsSAT-8	1.17
	IsSAT-9	1.24
	IsSAT-10	1.28
	IsSAT-11	1.4
	IsSAT-12	1.59

From the correlation between sample size and BTS (Eq. (5)), $BTS_{(54)}$ was calculated for all samples and plotted against I_{s50} as shown in Fig. 16:

$$BTS/BTS_{(54)} = 0.81\,(54/D)^{0.92} \quad (5)$$

In Fig. 16, the coefficient of determination (R^2) between BTS and PLI is very low (~0.35), meaning that the correlation is not reliable for use in practice. For this case, again the trend line was forced through the origin. It is worth mentioning that not forcing the line through zero increases the coefficient of determination to 0.82, changing the correlation to $BTS_{(54)} = 0.86I_{s50} + 4.3$ which is not preferred by the authors due to the lack of any physical explanations for the random y-intercept in the equation.

Heidari et al. (2012) conducted both axial and diametrical PLI tests on gypsum samples and reported that although diametrical PLI tests show a good correlation with UCS, there is a significant reduction in correlation between PLI and BTS. They attributed this reduced correlation to inhomogeneities in the gypsum samples, e.g. the presence of micrite veins or micro-flaws in the samples, since they act as a weakness plane. Failure planes of samples for BTS tests are shown in Fig. 17, which shows that they all split in half despite having variations in composition or bedding planes (gray veins of different materials which are mostly carbonates and shale) with

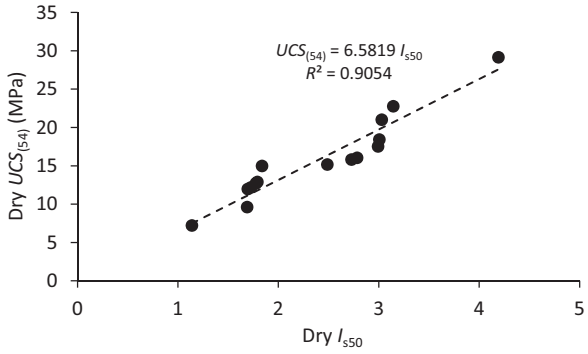

Fig. 12. $UCS_{(54)}$ vs. I_{s50} for air-dried samples.

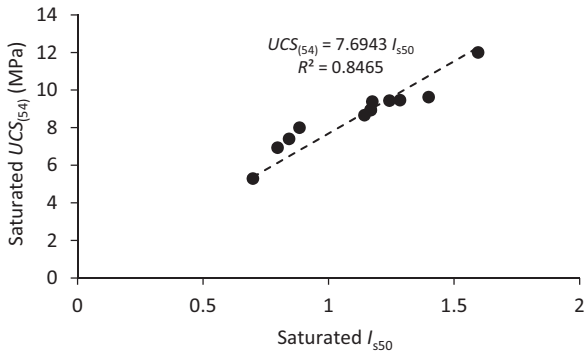

Fig. 13. $UCS_{(54)}$ vs. I_{s50} for saturated samples.

Table 7
Summary of BTS test results for dry and saturated samples.

Sample	ID	Diameter (mm)	*BTS* (MPa)	$BTS_{(54)}$ (MPa)
Air-dried	BTSDry-1	28.19	8.18	5.54
	BTSDry-2	28.19	9.06	6.15
	BTSDry-3	28.3	8.86	6.03
	BTSDry-4	28.15	8.87	6.01
	BTSDry-5	28.3	8.06	5.49
	BTSDry-6	28.29	8.07	5.49
	BTSDry-7	28.26	8.13	5.52
	BTSDry-8	28.2	7.84	5.32
	BTSDry-9	28.33	12.32	8.39
	BTSDry-10	28.49	11.76	8.05
	BTSDry-11	28.3	10.28	7
	BTSDry-12	54.2	5.71	7.06
	BTSDry-13	54.2	4.85	6.01
	BTSDry-14	53.98	7.93	9.78
	BTSDry-15	53.9	8.47	10.42
	BTSDry-16	54.04	6.95	8.57
	BTSDry-17	75.8	2.48	4.18
	BTSDry-18	75.9	2.85	4.81
	BTSDry-19	75.78	3.66	6.16
	BTSDry-20	75.74	3.65	6.15
	BTSDry-21	75.75	4.53	7.63
	BTSDry-22	75.81	3.45	5.81
	BTSDry-23	75.68	3.81	6.4
Saturated	BTSsat-1	75.69	1.95	
	BTSsat-2	75.47	1.99	
	BTSsat-3	75.51	1.42	
	BTSsat-4	75.59	2.22	
	BTSsat-5	75.91	2.85	
	BTSsat-6	75.92	2.53	
	BTSsat-7	75.76	2.82	
	BTSsat-8	54.33	5.05	
	BTSsat-9	53.41	2.95	

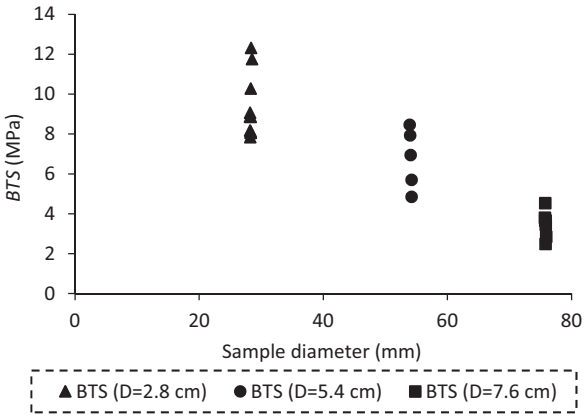

Fig. 14. BTS of samples with different diameters.

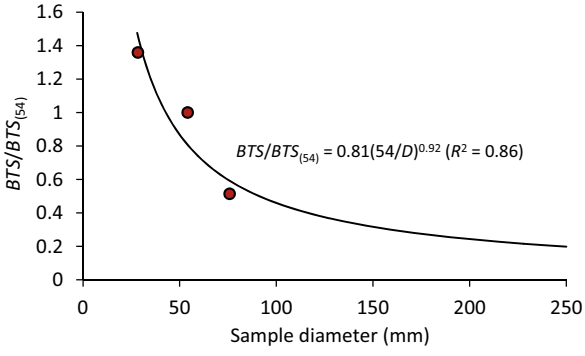

Fig. 15. Sample size effect on BTS of gypsum.

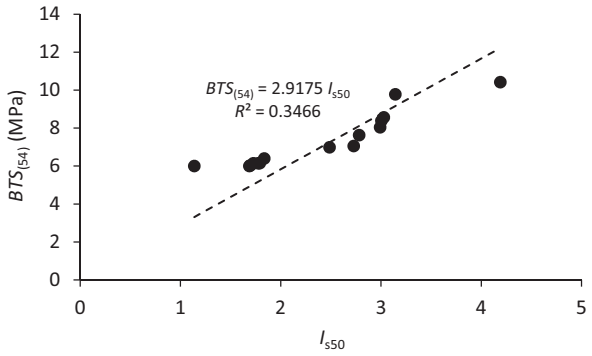

Fig. 16. Correlation between I_{s50} and $BTS_{(54)}$ for dry samples.

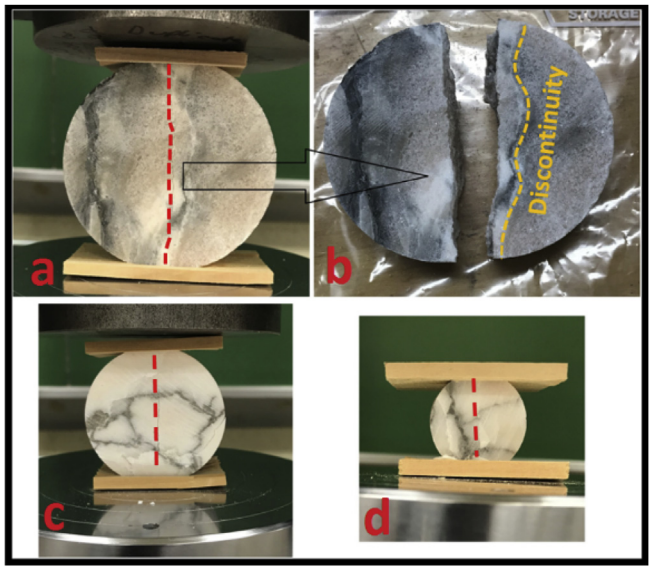

Fig. 17. Failure modes in BTS tests: the red dashed lines are drawn just next to the failure planes. (a) Sample with $D = 7.6$ cm, (b) Two separated sides of the sample "a" with the location of discontinuity just to the right of the failure plane highlighted with dashed yellow line, (c) Sample with $D = 5.4$ cm, and (d) Sample with $D = 2.8$ cm. The black veins (discontinuities) in samples "c" are almost perpendicular to the failure plane, while in sample "d", they are almost parallel to the failure plane.

different directions in respect to applied load. This indicates that heterogeneity of samples did not play an important role in failure. We suggest instead, however, that blast induced micro-flaws might be the key factor controlling the failure in the samples. Failure planes in PLI tests (as shown in Fig. 18) appeared to be independent of the direction of discontinuities. It is noted that independencies of failure mode and direction of discontinuities for sedimentary rocks have also been reported by Li and Wong (2012). They speculated that the low-grade metamorphism fuses the beddings of sedimentary rocks and prevents them from acting as weakness planes.

The BTS values of nine saturated samples were also tested (Table 7). The results were plotted against saturated I_{s50}, as shown in Fig. 19. As mentioned previously, there were not enough samples with different diameters to determine the size effect on the BTS of saturated gypsum, thus the correlation only represents the relationship between BTS of the samples with 7.6 cm diameter and I_{s50}. Although the coefficient of determination of 0.93 shows a high correlation between BTS and I_{s50}, it can be used only if the BTS is measured using samples with a 7.6 cm diameter.

Fig. 18. Failure modes in PLI tests on samples with discontinuities situated at different directions, in respect to the applied point load (sample b with no apparent discontinuity).

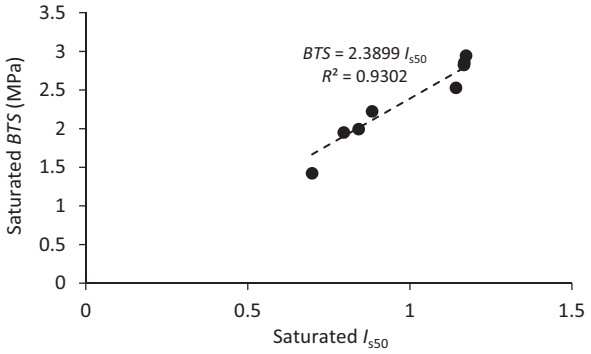

Fig. 19. Correlation between BTS of saturated samples with $D = 7.6$ cm and saturated I_{s50}.

4. Conclusions

Mechanical properties of Michigan Basin's gypsum in dry and saturated conditions were investigated in this study. Based on the results of this study, the following conclusions were drawn:

(1) For the gypsum samples from the Michigan Basin, the average standard UCS values, $UCS_{(54)}$, of dry and saturated gypsum samples were around 19 MPa and 11 MPa, respectively, indicating a 41% reduction due to the saturation. While these results are for blasted rock, $UCS_{(54)}$ of intact dry rock with minimum flaws can be as high as 29 MPa, and 18 MPa for intact saturated rock. These intact rock strengths were estimated by calculating the highest strength from the smallest samples ($D = 2.8$ cm) and converting it to $UCS_{(54)}$ using the equations derived in this study.

(2) The elasticity moduli of samples decreased by 30%–50% due to saturation.

(3) The PLI to UCS conversion factors of 6.6 for dry samples and 7.7 for saturated samples were measured for blasted gypsum from Michigan Basin.

(4) When the testing samples are in a wide range of sizes (e.g. samples used for UCS tests in this study), the scatter in the test results is more noticeable in smaller samples than in larger samples. This is because when preparing small samples, one sample could be prepared with minimum flaws while the concentration of flaws in another sample is high. In contrary, almost all of the large samples have a high amount of micro-flaws. On the other hand, the BTS test results tend to have less scatter since the range of sample sizes is smaller than that for UCS test.

(5) Scale effect on UCS of dry and saturated gypsum samples is different and can be presented using Eqs. (3) and (4). The size of the samples has a similar effect on BTS, which can be estimated using Eq. (5).

(6) While PLI and BTS of dry samples did not show a high correlation, a PLI to BTS conversion factor of 2.4 was found for saturated samples of 7.6 cm in diameter.

Conflicts of interest

We wish to confirm that there are no known conflicts of interest associated with this publication and there has been no significant financial support for this work that could have influenced its outcome.

Acknowledgments

We would like to thank the National City Quarry in Tawas, Michigan for providing the samples used in this research.

References

Ali SA. Creep properties of evaporite rocks with particular reference to gypsum. PhD Thesis. University of Sheffield; 1979.
ASTM D3967-16. Standard test method for splitting tensile strength of intact rock core specimens. West Conshohocken, PA, USA: ASTM International; 2016.
ASTM D4373-14. Standard test method for rapid determination of carbonate content of soils. West Conshohocken, PA, USA: ASTM International; 2014.
ASTM D5731-16. Standard test method for determination of the point load strength index of rock and application to rock strength classifications. West Conshohocken, PA, USA: ASTM International; 2016.
ASTM D7012-14. Standard test methods for compressive strength and elastic moduli of intact rock core specimens under varying states of stress and temperatures. West Conshohocken, PA, USA: ASTM International; 2014.
Basu A, Mishra DA, Roychowdhury K. Rock failure modes under uniaxial compression, Brazilian, and point load tests. Bulletin of Engineering Geology and the Environment 2013;72(3–4):457–75.
Bieniawski ZT. The point-load test in geotechnical practice. Engineering Geology 1975;9(1):1–11.
Castellanza R, Gerolymatou E, Nova R. An attempt to predict the failure time of abandoned mine pillars. Rock Mechanics and Rock Engineering 2007;41(3):377–401.
Chau KT. Analytic solutions for diametral point load strength tests. Journal of Engineering Mechanics 1998;124(8):875–83.
Doktan M. The long term stability of room and pillar workings in a gypsum mine. PhD Thesis. Department of Mining Engineering, University of Newcastle upon Tyne; 1983.
Doulati Ardejani F, Sadeghiamirshahidi M, Singh RN, Eslam Kish T, Reed SM. Prediction of the groundwater rebound process in a backfilled open cut mine using an artificial neural network. Mine Water and the Environment 2013;32(4):251–7.
Grimsley GP. Gypsum deposits in Michigan, gypsum deposits in the United States. United states department of the interior. Geological Survey. Bulletin No. 223, Series A, Economic Geology 1904:45–7.
Heidari M, Khanlari GR, Torabi Kaveh M, Kargarian S. Predicting the uniaxial compressive and tensile strengths of gypsum rock by point load testing. Rock Mechanics and Rock Engineering 2012;45(2):265–73.
Hoek E, Brown ET. Underground excavations in rock. London, UK: Institution of Mining and Metallurgy; 1980.
Hoxha D, Homand F, Auvray C. Deformation of natural gypsum rock: mechanisms and questions. Engineering Geology 2006;86(1):1–17.
Li D, Wong L. Point load test on meta-sedimentary rocks and correlation to UCS and BTS. Rock Mechanics and Rock Engineering 2012;46(4):889–96.
Lisk RD. The wet and dry strength of 'A' bed gypsum, Kirkby Thore, Cumbria. PhD Thesis. University of Newcastle upon Tyne; 1975.

Marolt Čebašek T, Frühwirt T. Investigation of creep behaviours of gypsum specimens with flaws under different uniaxial loads. Journal of Rock Mechanics and Geotechnical Engineering 2018;10(1):151–63.
Munoz H, Taheri A. Specimen aspect ratio and progressive field strain development of sandstone under uniaxial compression by three-dimensional digital image correlation. Journal of Rock Mechanics and Geotechnical Engineering 2017;9(4):599–610.
Preston K. The influence of water on the strength characteristics of gypsiferous rocks. PhD Thesis. University of Newcastle upon Tyne; 1980.
Sadeghiamirshahidi M, Vitton SJ. Methods of saturation and water content measurements for natural gypsum. Journal of Rock Mechanics and Geotechnical Engineering 2019a;11(2):219–27.
Sadeghiamirshahidi M, Vitton SJ. Laboratory study of gypsum dissolution rates for an abandoned underground mine. Rock Mechanics and Rock Engineering 2019. https://doi.org/10.1007/s00603-018-1696-6.
Salehin S. Investigation into engineering parameters of marls from Seydoon dam in Iran. Journal of Rock Mechanics and Geotechnical Engineering 2017;9(5):912–23.
Salih N, Mohammed A. Characterization and modeling of long-term stress–strain behavior of water confined pre-saturated gypsum rock in Kurdistan Region, Iraq. Journal of Rock Mechanics and Geotechnical Engineering 2017;9(4):741–8.
USGS. Maps, data and publications. U.S. Department of the Interior, U.S. Geological Survey. https://www.usgs.gov (accessed: 4/2/2018).
Vitton SJ. Final report on the risk assessment of the I-196 Interstate Section located over the former Domtar mine. Grand Rapids: Michigan Department of Transportation; 2004. Technical report SPR-1449.
Wong LNY, Jong MC. Water saturation effects on the Brazilian tensile strength of gypsum and assessment of cracking processes using high-speed video. Rock Mechanics and Rock Engineering 2014;47(4):1103–15.
Xie H, Pei J, Zuo J, Zhang R. Investigation of mechanical properties of fractured marbles by uniaxial compression tests. Journal of Rock Mechanics and Geotechnical Engineering 2011;3(4):302–13.
Yilmaz I. Influence of water content on the strength and deformability of gypsum. International Journal of Rock Mechanics and Mining Sciences 2010;47(2):342–7.
Yoshinaka R, Osada M, Park H, Sasaki T, Sasaki K. Practical determination of mechanical design parameters of intact rock considering scale effect. Engineering Geology 2008;96(3–4):173–86.
Yu Y, Zhang J, Zhang J. A modified Brazilian disk tension test. International Journal of Rock Mechanics and Mining Sciences 2009;46(2):421–5.

Mohammadhossein Sadeghiamirshahidi obtained his BSc degree in Mining Engineering from Yazd University, Iran, in 2007, and his MSc degree in Mining Engineering from Amirkabir University of Technology (Tehran Polytechnic), Tehran, Iran in 2011. He is currently a PhD candidate in Civil Engineering (Geotechnical Engineering) at Michigan Technological University. His research interests include (1) experimental investigations of soil and rock properties (especially dynamic and static mechanical properties), (2) slope stability and underground mine stability, mine pillar design and long-term stability, (3) acid mine drainage generation and mine-reclamation, and (4) intellectual, numerical and analytical modeling of the Earth systems.

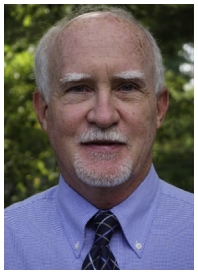

Stanley Vitton obtained his BSc and MSc degrees in Geological and Mining Engineering from Michigan Technological University, in 1976 and 1978, respectively, and his PhD in Civil Engineering from the University of Michigan, in 1994. He has eight years of industrial experience with the Shell Oil Company. While at Shell, Dr. Vitton was the Engineering Manager of their subsidiary the R&F Coal Company and a senior mining engineer on mining projects across the United States. His research is in the area of applied geomechanics specializing in blasting vibrations for both civil and mining engineering projects, high-strain rate dynamics of civil engineering materials, slope stability, and the analysis of the stability of abandoned surface and underground mines. Dr. Vitton is actively involved in a number of national and international research and educational activities related to civil engineering.